International Journal of Innovative Technology and Exploring Engineering (IJITEE)
ISSN: 2278-3075 (Online), Volume-7 Issue-1, September 2017

Analytical Study of Transient Magneto-Hydrodynamic Electroosomotic Flow and Heat Transfer Analysis in a Horizontal Channel

Asibor, Raphael E., Asibor Victor O.

Abstract: ***The research work focuses on transient magneto-hydrodynamic electro-osmotic flow and heat transfer analysis in a horizontal microchannel based on the linearized Helmholtz-Smoluchowski approximation and the Navier-Stokes equation. A numerical study of electroosmotic flow through horizontal channels is developed. The governing partial differential equations are transformed into a set of nonlinear coupled ordinary differential equations and solved by perturbation techniques. The effects of various physical parameters on the dimensionless velocity, temperature and concentration profiles are presented graphically, analysed and discussed in detail. The influences of fluid characteristics such as the skin friction coefficient, Nusselt and Sherwood numbers are discussed. Findings indicate that the governing flow parameters have significant influences on flow, heat and mass transfer characteristics.***

Keywords: ***Analytical study, electro-osmotic flow, Magneto-hydrodynamic, Microfluidics, Transient.***

I. INTRODUCTION

Electro-osmotic flow is the process in which an ionized liquid moves with respect to a stationary electrically charged surface under the action of an externally applied electric field. This phenomenon was first observed by Ruess in 1809 and in mid-19th century. Wiedemann formally proposed the mathematical theory behind it. In general, liquid motion can be generated by either applying a pressure gradient or imposing an electric field, leading to respective pressure-driven flow or electrokinetically-driven flow. Electroosmotic flow has an important effect at the microscale provide a viable alternative to pressure-driven liquid flow at microscales, with better flow control and no moving parts. The set of equations that describe MHD are a combination of the Navier-Stokes equations and Maxwell's equations.

The magneto-hydrodynamic (MHD) flow between two parallel plates, known as Hartmann flow, is a classical problem that has many applications in MHD power generators, MHD pumps, accelerators, aerodynamic heating, electrostatic precipitation, polymer technology, petroleum industry, purification of crude oil and fluid droplets and sprays. Many engineering problems are susceptible to MHD analysis. The study of MHD flow problems has achieved remarkable interest Magneto-drodynamic aspects of electroosmotic flow in microchannel were analyzed by Burgreen and Nakache (1964). Rice and Whitehead (1965) investigated fully developed electroosmotic flow in a narrow cylindrical capillary for low zeta potentials, using the Debye–Huckel linearization. Also, an analytical solution for electroosmotic flow in a cylindrical capillary was derived by Kang *et al*. (2002) by solving the complete Poisson–Boltzmann equation for arbitrary zeta-potentials.

Pressure-driven non-Newtonian flow has long been studied, the electroosmotic flow flow of a non-Newtonian fluid was not theoretically investigated until recently. Motivated to study biofluids in microsystems, Das and Chakraborty (2006), and Zimmerman *et al*. (2006) were among the first to present theoretical work on non-Newtonian electrokinetic flow and transport in microchannels. The non-Newtonian model adopted by Das and Chakraborty (2006) is the power-law model, while that by Zimmerman *et al*. (2006) is the Carreau model. The power-law (also known as Ostwald-de Waele) model is one of the simplest models to describe nonlinear viscous behaviors. It is a two-parameter model, where the shear-thinning or shear thickening behaviors can be conveniently represented by the flow index being less than or larger than 1, respectively.

Subsequently, this study presents an analytic and numerical solution of the transient magneto-hydrodynamic electro-osmotic flow of heat transfer analysis in a horizontal rectangular microchannel driven by an electric field. The numerical simulations coupled with perturbation method were carried out which is the numerical simulations of the solutions obtained using perturbation method were verified by the comparison with the available exact solutions for non-Newtonian fluids and examine effects of fluid rheology (fluid behavior index) on the transient velocity temperature and concentration distributions of the electro-osmotic flow of magneto-hydrodynamic fluids. Results are compared with the existing results and found good agreement with the results of Chamkha (2004). We derive expressions for the mean velocity, mean induced temperature and mean concentration. To the best knowledge of our knowledge mean velocity, mean temperate and mean concentration in microchannel under electro-osmotic flow (EOF) has not yet been studied.

Manuscript published on 30 September 2017.
***Correspondence Author(s)**
Dr Asibor Raphael Ehikhuemhen, Department of Computer Science/Information Technology, Igbinedion University/ College of Natural & Applied Sciences/ Organization Name, Okada, Nigeria, E-mail: asibor.raphael@iuokada.edu.ng
Mr Asibor Victor Osemudiamhen, Department of Physics, University ofAbuja, Abuja Nigeria, E-mail: asiborvictor292@gmail.com

II. MATHEMATICAL FORMULATION OF THE PROBLEM

The formation of electroosmotic flow in a straight microchannel is shown in figure 1. Here the channel walls attain net negative charges due to ionization, The length of the channel is L_0 while the width is assumed to much larger than the height, *H*, i.e., w >> 2H. The bottom plate is located at $y = -H$ while the top plate is located at $y = +H$. A potential is applied along the axis of the channel which provides the necessary driving force for the flow.

A. Assumptions and approximations

The main simplifying assumptions and approximations in our analysis are as follows:

I. The fluid viscosity is independent of the local electric field strength. This condition is an approximation. Since the ion concentration and the electric field strength within the EDL are increased, the viscosity of the fluid may be affected.

II. The Poisson–Boltzmann equation is valid when the ion convection effects are negligible. Hence, our analysis is valid for Stokes flows, or for hydraulically fully developed channel flows. The solvent is continuous, and its permittivity is not affected by the overall and the local electric field strength.

III. No pressure driven component is present in the velocity distribution and the ions are point charges.

The governing equations of the model based on the assumptions above are:

Equation of Continuity

$$\frac{\partial v^*}{\partial y^*} = 0 \qquad 1$$

Equation of Momentum

$$\frac{\partial u^*}{\partial t^*} + v^* \frac{\partial u^*}{\partial y^*} = \nu \frac{\partial^2 u^*}{\partial y^{2*}} - \frac{1}{\rho}\frac{\partial p}{\partial x} + \frac{g\beta}{\rho}\left(T^* - T_\infty\right) + \frac{g\beta}{\rho}\left(\psi^* - \psi_\infty\right) + \frac{\rho_e E_x}{\rho} u^* - \frac{\delta B_0^{\,2}}{\rho} u^* \qquad 2$$

Equation of Energy

$$\frac{\partial T^*}{\partial t^*} + v^* \frac{\partial T^*}{\partial y^*} = \alpha \frac{\partial^2 T^*}{\partial y^{2*}} - \frac{1}{\rho c_p}\frac{\partial q_r^{\,*}}{\partial y^*} + \frac{Q_0}{\rho c_p}\left(T^* - T_\infty\right) + \frac{Q_1}{\rho c_p}\left(\psi^* - \psi_\infty\right) \qquad 3$$

Equation of Mass Diffusion

$$\frac{\partial \psi^*}{\partial t^*} + v^* \frac{\partial \psi^*}{\partial y^*} = D \frac{\partial^2 \psi^*}{\partial y^{2*}} - Kr^*\left(\psi^* - \psi_\infty\right) \qquad 4$$

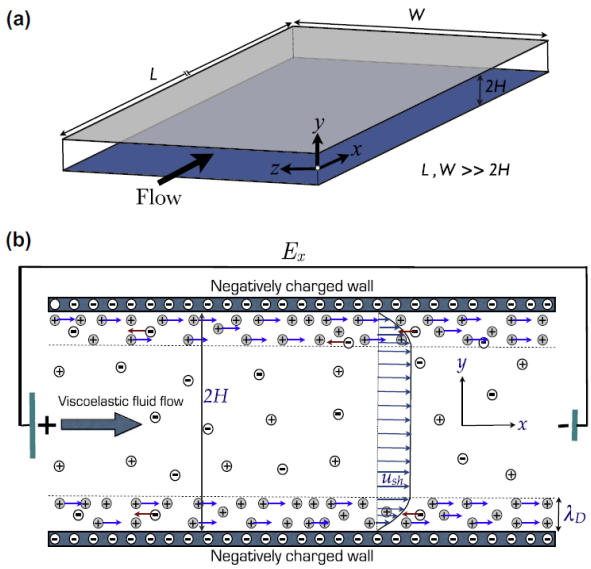

Figure 1. (a) Diagram of the microchannel considered in this paper; (b) 2D representation of electro osmotic flow *(Dhinakaran et al., 2010).*

It is convenient to employ the following dimensionless variables where, x, y and t are the dimensional distances along and perpendicular to the plate and dimensional time, respectively. u and v are the components of dimensional velocities along x and y directions, ρ is the fluid density, μ is the viscosity, C_p is the specific heat at constant pressure, σ is the fluid electrical conductivity, B_0 is the magnetic induction, T is the dimensional temperature, k is the thermal conductivity of the fluid. The appropriate and corresponding initial and boundary condition for velocity, temperature and concentration fields are given as follows:

$$u(\pm h,t) = 0, \qquad T(\pm h,t) = 0 \qquad \psi(\pm h,t) = \delta_0 \qquad 5$$

$$u(y,0) = T(y,0) = \psi(y,0) = 0 \qquad v(0,t) = v(t) \qquad 6$$

where mean stream velocity, $\cup = 1 + \varepsilon e^{iwt}$ 7

and at free stream velocity, $u = u(t)$. It is clear from equation 7 that the suction velocity at the plate surface is a function of time only. Integrating the continuity equation 1 and with equation 7 assuming that it takes the exponential form, we have

$$v^* = -v_0\left(1 + \varepsilon A e^{nt}\right) \qquad 8$$

Since the suction velocity is normal to the plate and it is a function of time only, it is convenient to take the following exponential form where A is a real positive constant, ε and εA are small quantities less than unity, and v_0 is a scale of suction velocity which has non-zero positive constant $(v_0 > 0)$.

Published By:
Blue Eyes Intelligence Engineering
and Sciences Publication (BEIESP)

It is convenient to employ the following non- dimensionless quantities and if we follow Messiha (1966) equations (2 - 4) becomes

$$v(y,t) = v(t) = -v_0\left(1+\in Ae^{nt}\right) = -v_0\left(1+\varepsilon Ae^{\frac{v_0^2 n'}{4\nu}\cdot\frac{4\nu}{v_0^2}t'}\right) = -v_0\left(1+\varepsilon Ae^{n't'}\right) \quad 9$$

where, A is a real positive constant, ε and εA are small less than unity, ($\in A << 1$) and v_0 is a scale of suction velocity which has non-zero positive constant. Under these assumptions, the appropriate boundary conditions for the velocity, temperature and concentration fields are

$$u = u_p, \quad \theta_0 = 1+\varepsilon e^{nt}, \quad \psi = 1+e^{nt}, \quad at \quad y = 0$$
$$u \to 0, \quad \theta \to 0, \quad \psi \to 0, \quad \text{as} \quad y \to \infty$$

It is convenient to employ the following dimensionless variables

$$u = \frac{u^*}{V_0}, \quad v = \frac{v^*}{V_0}, \quad \nu = \frac{\mu}{\rho}, \quad y = \frac{V_0 y^*}{\nu}, \quad t = \frac{V_0^2 t^*}{\nu},$$

$$k = \frac{V_0^2 k^*}{\nu^2}, \qquad Kr = \frac{\nu K_r^*}{V_0^2}, \qquad \Pr = \frac{\nu\rho c_p}{k} = \frac{\nu}{\alpha},$$

$$\theta = \frac{T^* - T_\infty^*}{T_w^* - T_\infty^*}, \qquad \phi = \frac{\psi^* - \psi^*_\infty}{\psi^*_w - \psi^*_\infty}$$

$$Gr = \frac{\nu g\beta_T\left(\bar{T}_w - \bar{T}_\infty\right)}{U_o V_0^2}, \quad Gm = \frac{\nu g\beta_\psi\left(\bar{\psi}_w - \bar{\psi}_\infty\right)}{U_o V_0^2},$$

$$S_c = \frac{\nu}{D_m}, \qquad S_0 = \frac{D_1}{\nu}\frac{\left(T_w^* - T_\infty^*\right)}{\left(\psi_w^* - \psi_\infty^*\right)}, \qquad M = \frac{\sigma B_0^2 \nu}{\rho V_0^2},$$

$$Q = \frac{\nu Q_o}{\rho c_p V_o^2}, \quad R = \frac{\nu Q_1}{\rho c_p V_o^2}, \quad \chi = \frac{Q_1 \nu\left(\psi_w^* - \psi_\infty^*\right)}{\rho c_p V_0^2\left(T_w^* - T_\infty^*\right)},$$

$$\lambda = \frac{2ev Z^2 n_0 \varsigma}{\rho V_0^2 k_B T}\nabla\varphi, \; n = \frac{n^*\nu}{V_o^2}, \; N = M - \lambda,$$

u, v velocity profile
θ temperature
C' Dimensional concentration of the fluid
ψ Constant concentration at the plate
Gm solutal Grashof number
Gr Thermal Grashof number
$\Pr$ Prandtl number
Kr Chemical reaction parameter
Sc Schmidt number
So Soret number
χ modified Durfour number
M magnetic parameter (Hartmann number)
λ electroosmotic parameter
Q Dimensional heat generation term
R heat generation term
Q_0 heat generation parameter
Q_1 heat generation parameter
t Dimensionless time
t_0 Characteristic time
t' Dimensional time
U Dimensionless velocity of the fluid
U' Dimensional velocity of the fluid
y Dimensionless co-ordinate perpendicular to the plate

(10)

$$\rho_e = -\frac{2z^2 e^2 n_0 \xi}{k_B T}, \qquad 12$$

Where z the valence of ions is, e is the fundamental charge, k_B is the Boltzmann constant, T is the absolute temperature. With the help of the Debye-Huckel approximation

$$\rho_e E_x = \kappa^2 \xi\left(E_x\right) = -\kappa^2 \varepsilon\xi E_x \qquad 13$$

Here $\kappa = \left(\frac{2z^2 e^2 n_0}{\varepsilon k_B T}\right)^{\frac{1}{2}}$ is the Debye-Huckel parameter and κ^{-1} means the thickness of EDL

$$\frac{\partial u^*}{\partial t^*} + v^*\frac{\partial u^*}{\partial y^*} = \nu\frac{\partial^2 u^*}{\partial y^{2*}} + \frac{g\beta}{\rho}\left(T^* - T_\infty\right) + \frac{g\beta}{\rho}\left(\psi^* - \psi_\infty\right) + \frac{1}{\rho}\left[\kappa^2 \varepsilon\xi E_x\right]u^* + \frac{\delta B_0^2}{\rho}u^*$$

14

If the Debye length is small compared with the channel width, then the curvature terms can be neglected and Using the Poisson Boltzmann approximation, equation 13 reduces to the one-dimensional form appropriate to the electroosmotic flow past a long plane channel.

$$-2eZn_0 \sinh\left(\frac{eZ\varsigma}{k_B T}\right)\Delta\varphi = \frac{2eZ^2 n_0 \varsigma}{k_B T}\nabla\varphi \qquad 15$$

In summary, equations 14, 3 and 4 form the system of equations to be solved

$$\frac{\partial u}{\partial t} - \left(1+\varepsilon Ae^{nt}\right)\frac{\partial u}{\partial y} = \frac{\partial^2 u}{\partial y^2} + Gr\theta + Gm\phi - Nu \quad 16$$

Published By:
Blue Eyes Intelligence Engineering
and Sciences Publication (BEIESP)

$$\frac{\partial\theta}{\partial t}-\left(1+\varepsilon Ae^{nt}\right)\frac{\partial\theta}{\partial y}=\frac{1}{\Pr}\frac{\partial^2\theta}{\partial y^2}-Q\theta+\chi\phi \qquad 17$$

$$\frac{\partial\phi}{\partial t}-\left(1+\varepsilon Ae^{nt}\right)\frac{\partial\phi}{\partial y}=\frac{1}{S_c}\frac{\partial^2\phi}{\partial y^2}-k_r\phi \qquad 18$$

with the following dimensionless boundary conditions.

$$u_0=u_1=u_\infty=0,\ \theta_0=\theta_1=1,\quad \phi_0=1,\quad h_1=1 \quad at\ y=0$$

$$u_0=u_1\to 0,\quad \theta_0\to 0,\theta_1\to 1,\quad \phi_0\to 0,\quad h_1\to 0 \quad as\ \ y\to\infty$$

III. METHOD OF SOLUTIONS

To solve for low values of equations (16), (17) and (18) subject to the boundary conditions (19), we use the following linear transformations (**Kim and Lee, 2003**) to split each equation into harmonic and non-harmonic parts. Equations (16), (17) and (18) represent a set of partial differential equations that cannot be solved in closed form. However, it can be reduced to a set of ordinary differential equations in dimensionless form that can be solved analytically. This can be done, by representing the velocity, temperature and concentration in terms of harmonic and non-harmonic functions as in (Okoro *and Asibor*, 2016) as follows:

$$u(y,t)=f_0(y)+\varepsilon e^{nt}f_1(y)+0\left(\varepsilon^2\right) \qquad (20)$$

$$\theta(y,t)=g_0(y)+\varepsilon e^{nt}g_1(y)+0\left(\varepsilon^2\right) \qquad (21)$$

$$\phi(y,t)=h_0(y)+\varepsilon e^{nt}h_1(y)+0\left(\varepsilon^2\right) \qquad (22)$$

Substituting equations (20) - (22) into equation (16), equation (17) and equation (18) equating the harmonic and non-harmonic terms, and neglecting and higher- order terms of $0\left(\varepsilon^2\right)$ We have

$$f_0''(y)+f_0'(y)-Nf_0(y)=-G_rg_0(y)-G_mh_0(y) \qquad (23)$$

$$g_0'(y)+\Pr g_0(y)-\Pr Qg_0(y)=-\Pr\chi h_0(y) \qquad (24)$$

$$h_0''+S_ch_0'-S_cK_rh_0=0 \qquad (25)$$

$$f_1''+f_1'-(N+n)f_1=-Af_0'-G_rg_1-G_mh_1 \qquad (26)$$

$$g_1''+\Pr g_1'-\Pr(Q+n)g_1=-A\Pr g_0'-\Pr\chi h_1 \qquad (27)$$

$$h_1''+Sch_1'-(k_r+n)S_ch_1=-AS_ch_0' \qquad (28)$$

To obtain a solution of the Naiver-Stokes equations that suits a particular problem like equation (23 – 28), it is necessary to add conditions that need to be satisfied on the boundaries of the region of interest in this thesis, we use following boundary conditions:

$$f_0=f_1=u_p=0,\ g_0=g_1=1,\quad h_0=h_1=1,\quad at\ y=0$$

$$f_0=f_1\to 0,\quad g_0\to 0,g_1\to 0,\ h_0\to h_1\to 0,\quad as\ \ y\to\infty$$

This singularity is solved with consideration of entrance effect at the initial stage of filling, as discussed in recent studies (Chakraborty, 2007, **Chakraborty and Mittal, 2007**, Huang et al., 2001, Chakraborty, 2005). In this investigation, as the asymptotic solution is considered, the equations (428, 4.73 and 4.127) is acceptable.

$$\phi(y,t)=h_0(y)+\varepsilon e^{nt}h_1(y)+0\left(\varepsilon^2\right)$$

$$\phi(y,t)=C_1e^{-m_2y}+\varepsilon e^{nt}\left[C_3e^{-m_2y}+\left(1-C_3\right)e^{-m_1y}\right] \qquad (29)$$

$$\theta(y,t)=g_0(y,t)+\varepsilon e^{nt}g_1(y,t)+O(\varepsilon^2)$$

$$\theta(y,t)=C_5e^{-m_3y}+\left(1-C_5\right)e^{-m_1y}+\varepsilon e^{nt}\left[C_7e^{-m_4y}+C_9e^{-m_3y}+C_{10}e^{-m_2y}+C_{11}e^{-m_1y}\right] \qquad (30)$$

$$u(y,t)=C_{12}e^{-m_5y}+C_{14}e^{-m_1y}+C_{15}e^{-m_3y}+\varepsilon e^{nt}\left[\begin{matrix}C_{16}e^{-m_6y}+C_{18}e^{-m_1y}+C_{19}e^{-m_2y}+C_{20}e^{-m_3y}+\\C_{21}e^{-m_4y}+C_{22}e^{-m_5y}\end{matrix}\right] \qquad (31)$$

Skin friction

Knowing the velocity field, the skin friction at the wall can be obtained, which in non-dimensional form is given by

$$C_f=\frac{\tau_w'}{\rho U_0V_0}=\left(\frac{\partial u}{\partial y}\right)_{y=0}=\left(\frac{\partial u_0}{\partial y}+\varepsilon e^{nt}\frac{\partial u_1}{\partial y}\right)_{y=0} \qquad 32$$

$$u(y,t)=C_{12}e^{-m_5y}+C_{14}e^{-m_1y}+C_{15}e^{-m_3y}+\varepsilon e^{nt}\left[\begin{matrix}C_{16}e^{-m_6y}+C_{18}e^{-m_1y}+C_{19}e^{-m_2y}+C_{20}e^{-m_3y}+\\C_{21}e^{-m_4y}+C_{22}e^{-m_5y}\end{matrix}\right]$$

$$\left(\frac{\partial u_0}{\partial y}+\varepsilon e^{nt}\frac{\partial u_1}{\partial y}\right)=-m_5C_{12}e^{-m_5y}-m_1C_{14}e^{-m_1y}-m_3C_{15}e^{-m_3y}-\varepsilon e^{nt}\left[\begin{matrix}m_6C_{16}e^{-m_6y}+m_1C_{18}e^{-m_1y}+m_2C_{19}e^{-m_2y}+\\m_3C_{20}e^{-m_3y}+m_4C_{21}e^{-m_4y}+m_5C_{22}e^{-m_5y}\end{matrix}\right]$$

Published By:
Blue Eyes Intelligence Engineering
and Sciences Publication (BEIESP)

$$\left(\frac{\partial u_0}{\partial y}+\varepsilon e^{nt}\frac{\partial u_1}{\partial y}\right)_{y=0}=-m_5C_{12}-m_1C_{14}-m_3C_{15}$$

$$-\varepsilon e^{nt}\left[m_6C_{16}+m_1C_{18}+m_2C_{19}+m_3C_{20}+m_4C_{21}+m_5C_{22}\right]$$

Nusselt number

Knowing the temperature field, the heat transfer coefficient can be obtained which in the non-dimensional form, in terms of the Nusselt number, is given by

$$Nu=-x\frac{\left(\frac{\partial T'}{\partial y'}\right)}{T_w'-T_\infty'}\Rightarrow N_u\,\mathrm{Re}_x^{-1}=\left(\frac{\partial\theta}{\partial y}\right)_{y=0}$$

$$=\left(\frac{\partial\theta_0}{\partial y}+\varepsilon e^{nt}\frac{\partial\theta_1}{\partial y}\right)_{y=0}$$

$$\theta(y)=C_5e^{-m_3y}+(1-C_5)e^{-m_1y}+$$
$$\varepsilon e^{nt}\left[C_7e^{-m_4y}+C_9e^{-m_3y}+C_{10}e^{-m_2y}+C_{11}e^{-m_1y}\right] \quad 34$$

$$\frac{\partial\theta_0}{\partial y}+\varepsilon e^{nt}\frac{\partial\theta_1}{\partial y}=-m_3C_5e^{-m_3y}-m_1(1-C_5)e^{-m_1y}$$

$$-\varepsilon e^{nt}\left[m_4C_7e^{-m_4y}+m_3C_9e^{-m_3y}+m_2C_{10}e^{-m_2y}+m_1C_{11}e^{-m_1y}\right]$$

$$\left(\frac{\partial\theta_0}{\partial y}+\varepsilon e^{nt}\frac{\partial\theta_1}{\partial y}\right)_{y=0}=-m_3C_5-m_1(1-C_5) \quad (35)$$

$$-\varepsilon e^{nt}\left[m_4C_7+m_3C_9+m_2C_{10}+m_1C_{11}\right]$$

Sherwood number

The rate of mass transfer at the wall which is the ratio of length scale to the diffusive boundary layer thickness. Knowing the concentration field, the mass transfer rate can be obtained which in the non-dimensional form, in terms of the Sherwood t number, is given by

$$S_h=-x\frac{\left(\frac{\partial C'}{\partial y'}\right)_{y'=0}}{C_w'-C_\infty'}\Rightarrow S_h\,\mathrm{Re}_x^{-1}=\left(\frac{\partial C_0}{\partial y}+\varepsilon e^{nt}\frac{\partial C_1}{\partial y}\right)_{y=0}$$

$$\phi(y,t)=C_1e^{-m_2y}+\varepsilon e^{nt}\left[C_3e^{-m_2y}+(1-C_3)e^{-m_1y}\right]$$

$$\frac{\partial C_0}{\partial y}+\varepsilon e^{nt}\frac{\partial C_1}{\partial y}=-m_2C_1e^{-m_2y}$$

$$-\varepsilon e^{nt}\left[m_2C_3e^{-m_2y}+m_1(1-C_3)e^{-m_1y}\right]$$

$$\left(\frac{\partial C_0}{\partial y}+\varepsilon e^{nt}\frac{\partial C_1}{\partial y}\right)_{y=0}=m_2C_1-\varepsilon e^{nt}\left[m_2C_3+m_1(1-C_3)\right] \quad (36)$$

IV. MODEL VERIFICATION

To get a clear insight of the physical problem, the velocity, temperature and concentration have been discussed by assigning numerical values to the parameters encountered in the problem. To be realistic, the values of the embedded parameters were chosen following, Okoro and Asibor (2016), Ibrahim and Makinde (2011), Ibrahim and Makinde (2010); The values of Schmidt number (*Sc*) are chosen for hydrogen (*Sc* = 0.22), water vapour (*Sc* = 0.62), ammonia (*Sc* = 0.78) and Propyl Benzene (*Sc* = 2.62) at temperature 25◦C and one atmospheric pressure. The values of Prandtl number is chosen to be *Pr* = 0.71 which represents air at temperature 25◦C and one atmospheric pressure. Attention is focused on positive values of the buoyancy parameters i.e. Grashof number *Gr* > 0 (which corresponds to the cooling problem) and solutal Grashof number *Gc* > 0 (which indicates that the chemical species concentration in the free stream region is less than the concentration at the boundary surface).

Velocity profiles

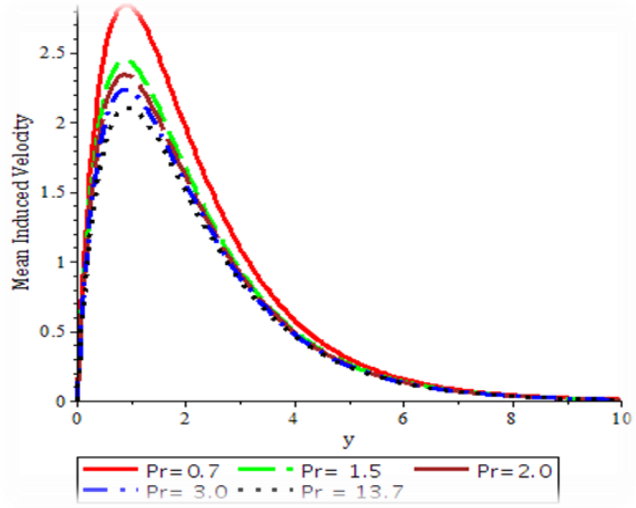

Figure 2: Effects of variation of prandtl numbers on mean velocity profile for fixed Sc, Kr, Q, Gr and Gm. (Sc= 0.26, a = 1.0, Kr = 1.0, n = 0.2, Q = 1, t = 0.2, χ = 0.7, ε = 0.0001, Gr = 7, Gm = 5 and N = 1.0.)

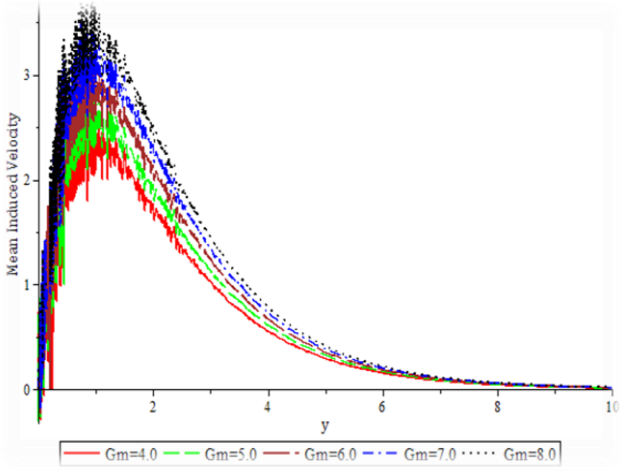

Figure 3: Effects of variation of solutal grasshoff numbers on mean velocity profile for fixed Sc, Kr, Q, Gr and Gm Sc= 0.26, a = 1.0, Kr = 1.0, n = 0.2, Q = 1, t = 0.2, χ = 0.7, ε = 0.0001, Gr = 7, Pr 1 and N = 1.0.

Published By:
Blue Eyes Intelligence Engineering
and Sciences Publication (BEIESP)

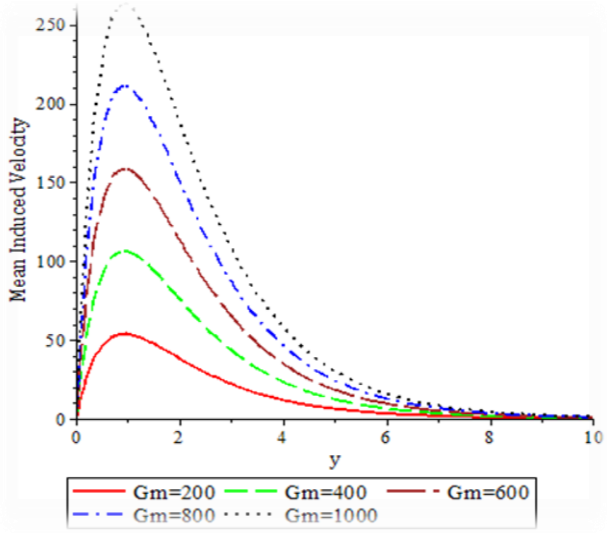

Figure 4: Effects of variation of increasing solutal grasshoff numbers on mean velocity profile for fixed Sc, Kr, Q, Gr and Gm Sc= 0.26, a = 1.0, Kr = 1.0, n = 0.2, Q = 1, t = 0.2, χ = 0.7, ε = 0.0001, Gr = 7, Pr 1 and N = 1.0.

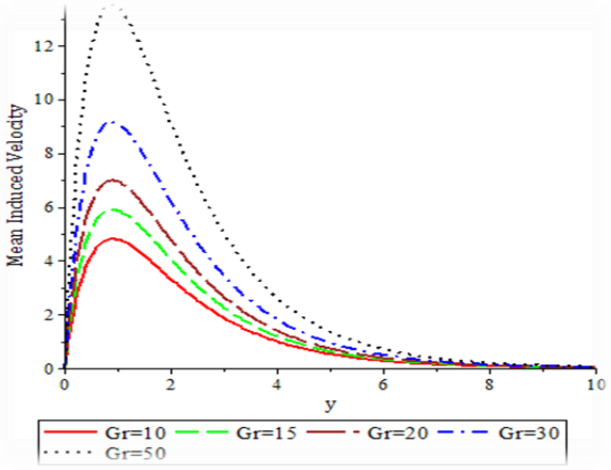

Figure 5: Effects of variation of grasshoff numbers on mean induced velocity profile for fixed Sc, Kr, Q, Gr and Gm Sc= 0.26, a = 1.0, Kr = 1.0, n = 0.2, Q = 1, t = 0.2, χ = 0.7, ε = 0.0001, Gm = 10, Pr 0.71 and N = 1.0

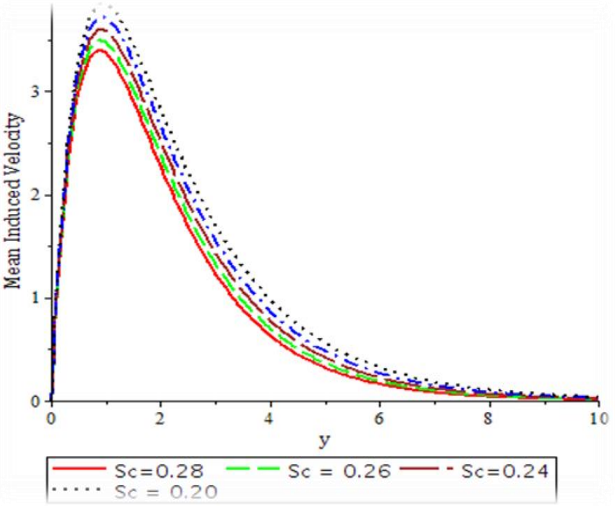

Figure 6: Effects of variation of Schmidt numbers on mean velocity profile for fixed Sc, Kr, Q, Gr and Gm a = 1.0, Kr = 1.0, n = 0.2, Q = 1, t = 0.2, χ = 0.7, ε = 0.0001, Gm = 5, Gr = 10, Pr 0.71 and N = 1.0

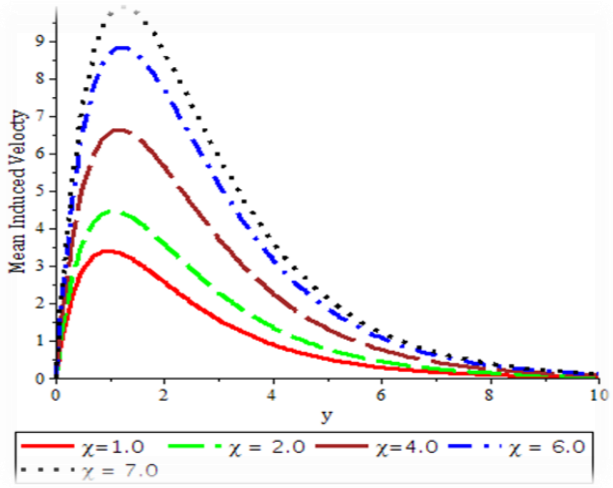

Figure 7: Effects of variation of modified dufour numbers on mean velocity profile for fixed Sc, Kr, Q, Gr and Gm a = 1.0, Q = 1.0, n = 0.2, Kr= 1.0, t = 0.2, Sc = 0.26, ε = 0.0001, Gm = 5, Gr = 10, Pr 0.71 and N = 1.0

Temperature Profile

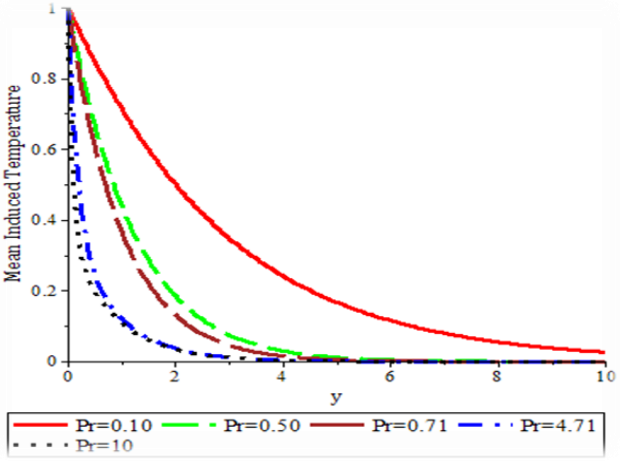

Figure 8: Effects of variation Prandtl numbers on mean temperature profile for fixed Sc, Kr, Q, Gr and Gm. a = 1.0, Q = 1.0, n = 0.2, Kr = 1.0, t = 0.2, Sc = 0.26, ε = 0.0001, t = 0.2. and χ = 0.7.

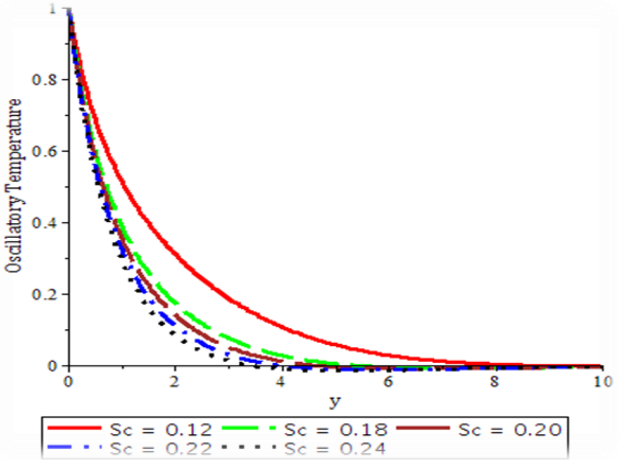

Figure 9: Effects of variation Schmidt numbers on temperature profile for fixed Sc, Kr, Q, Gr and Gm a = 1.0, Q = 1.0, n = 0.2, Kr = 1.0, t = 0.2, Sc = 0.26, ε = 0.0001, t = 0.2. and χ = 0.7.

Published By:
Blue Eyes Intelligence Engineering and Sciences Publication (BEIESP)

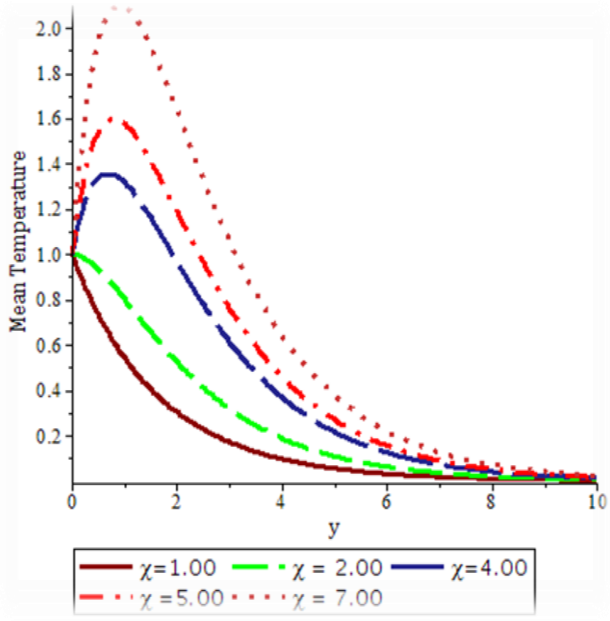

Figure 10: Effects of variation modified dufour numbers on mean temperature profile for fixed Sc, Kr, Q, Gr and Gm a = 1.0, Pr = 1.0, n = 0.2, Kr = 1.0, t = 0.2, Sc = 0.26, ε = 0.0001, t = 0.2. and χ = 0.7.

Concentration Profile

The concentration profile is shown in Fig. 11 - 13 for various parameters involved in the solution. Fig. 11 illustrates that fluid concentration increases with an increase in chemical reaction parameter Kr number it is because of the reason that a rise in Kr number causes a greater chemical thermal diffusivity. It is also clear from the same figure that with an increase in Schmidt number concentration

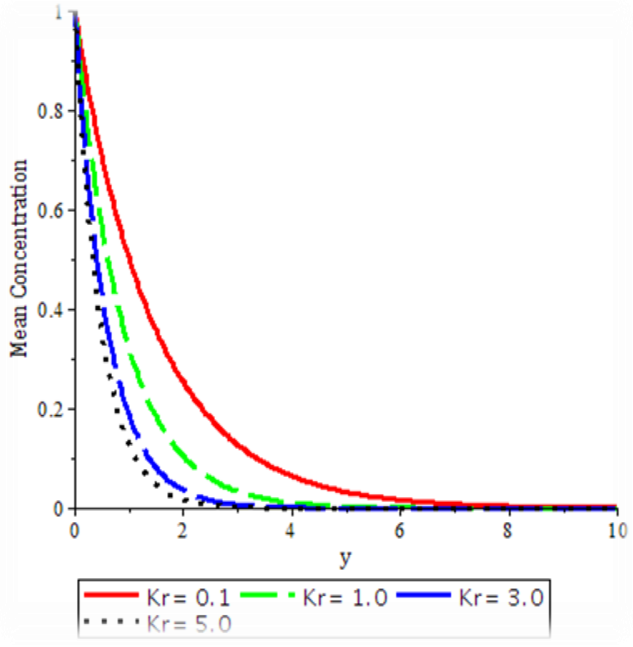

Figure 11: Effects of variation chemical reaction parameter on concentration profile for fixed Sc, Kr, Q, Gr and Gm. a = 1.0, n = 0.2, t = 0.2, Sc = 0.26, ε = 0.01, t = 0.2. and χ = 0.7.

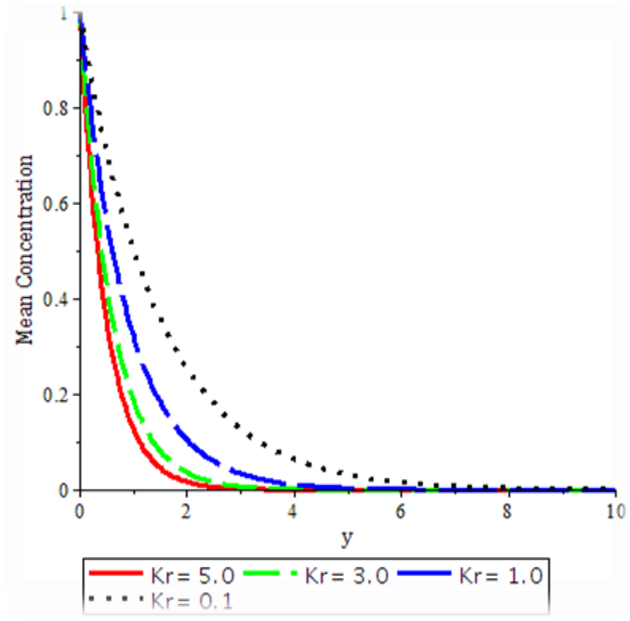

Figure 12: Effects of variation reducing chemical reaction parameter on concentration profile for fixed Sc, Kr, Q, Gr and Gm. a = 1.0, n = 0.2, t = 0.2, Sc = 0.26, ε = 0.01, t = 0.2. and χ = 0.7.

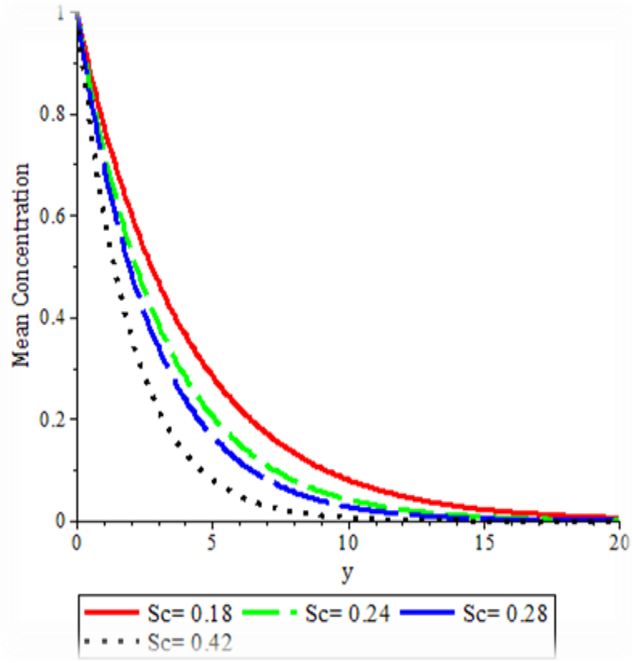

Figure 13: Effects of variation Schmidt number on concentration profile for fixed Sc, Kr, Q, Gr and Gm. a = 1.0, n = 0.2, t = 0.2, Sc = 0.26, ε = 0.01, t = 0.2. and χ = 0.7.

Equation (33), Equation (35) and Equation (36) represents the Skin friction, the Nusselt number and the Sherwood number respectively. They are analytically and numerically computed for different standard values, in estimating the velocity temperature and concentration impart at the surface channel our results are presented graphically showing the appropriate values.

Published By:
Blue Eyes Intelligence Engineering
and Sciences Publication (BEIESP)

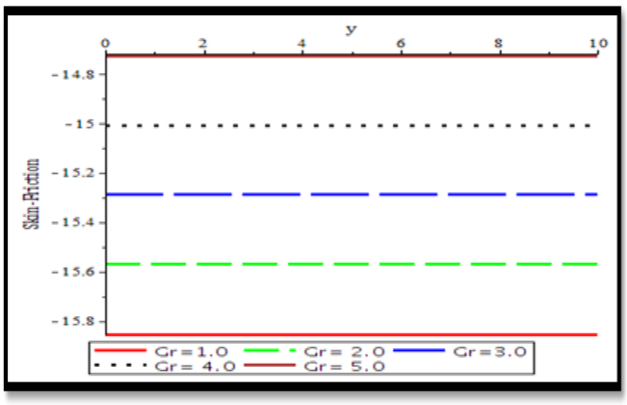

Figure 14. The Effect of Thermal Grass of number on Skin-friction

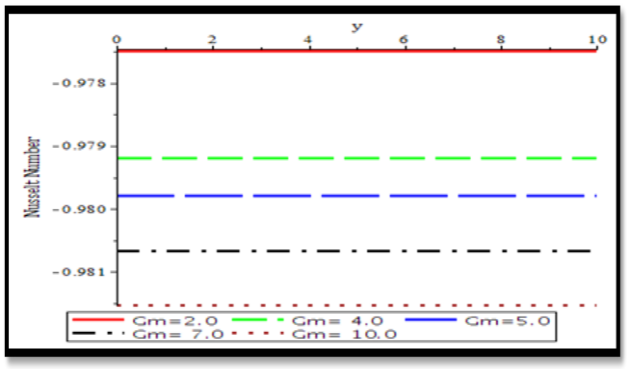

Figure 15. The Effect of Solutal Grass of number on Nusselt number

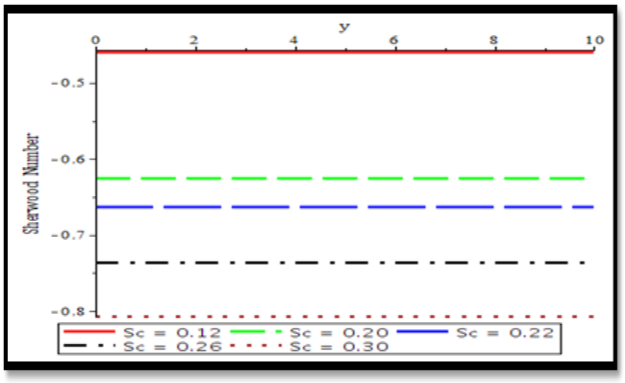

Figure 16. The Effect of modified Schimidt on Sherwood number

Taking account of this additional saving in the CPU time, one can expect that the current solution is far more efficient than what is already revealed in (Chamkha, 2004). It should be mentioned that all these calculations are performed on Maple 18.

V.CONCLUSION AND RECOMENDATIONS

Analytically transient magneto-hydrodynamic electroosmotic flow and heat transfer analysis in a rectangular horizontal microchannel by using perturbation technique are studied. For the case of transient electroosmotic flow, electric field drives the fluid within the double layer. The momentum of the double layer gradually transfer to the central region, and finally occupying the entire channel. The greater fluid behaviour index causes the fluid to respond more promptly to the influence of the applied electric field. The model calculation confirms that the velocity given in the previous works by Makinde and Chinyoka, 2010; Okedoye and Asibor, 2014. for a parallel plate is still valid for microchannels with rectangular/horizontal cross-sections. The velocity is of practical importance in non-Newtonian microfluidic manipulations adopting electroosmosis. In summary, comparison of the present result with the analytical solution, for the flow of non-Newtonian fluids available in the literature is found to be consistent and results can be effectively utilized for optimum design of microfluidic systems of practical interest.

REFERENCES

1. Burgreen, D. and Nakache, F. R. (1964). Electrokinetic flow in ultrafine capillary slits. Journal of Physical Chemistry, 68: 1084-1091.
2. Chakraborty, S. (2007). Electro-osmotically driven capillary transport of typical non-Newtonian biofluids in rectangular microchannels. Analytica Chimica Acta, 605: 175-184.
3. Chakraborty, S. (2005). Dynamics of capillary flow of blood into a microfluidic channel. Lab on a Chip - Miniaturisation for Chemistry and Biology, 5: 421-430.Chamkha
4. , A. J. (2004). “Unsteady MHD convective heat and mass transfer past a semi infinite vertical permeable moving plate with heat absorption”, Int. J. Engg. Sci., 42: 217-230. DOI: 10.1016/s0020-7225(03)00285-4.
5. Das, S. and Chakraborty, S (2006). Analytical solutions for velocity, temperature and concentration distribution in electro-osmotic microchannel flows of a non-Newtonian bio-fluid. Analytica Chimica Acta, 559: 15-24.
6. Debye, P. and Hückel, E. (1923). The theory of electrolytes. I. Lowering of freezing point and related phenomena. Physikalische Zeitschrift, 24: 185–206.
7. Dhinakaran, S., Afonso, A. M., Alves, M. A. and Pinho, F. T. (2010). Steady viscoelastic fluid flow between parallel plates under electro-osmotic forces: Journal of Colloid and Interface Science, **344**: 513–520.
8. Huang, W., Bhullar, R. S. and Yuan-cheng, F. (2001). The surface-tension-driven flow of blood from a droplet into a capillary tube. Journal of Biomechanical Engineering, 123: 446-454.
9. Ibrahim, S. Y. and Makinde, O. D. (2011). Chemically Reacting Magneto-hydrodynamics (MHD) Boundary Layer Flow of Heat and Mass Transfer past a Low-Heat-Resistant Sheet Moving Vertically Downwards. Scientific Research and Essays, 6(22): 4762-4775.
10. Ibrahim, S. Y. and Makinde, O. D. (2010). Chemically Reacting MHD Boundary Layer flow of Heat and Mass Transfer over a Moving Vertical Plate with Suction. Scientific Research and Essays. 5(19): 2875-2882.
11. Makinde, O. D. and Chinyoka, T. (2010). MHD transient flows and heat transfer of dusty fluid in a channel with variable physical properties and Navier slip condition, Computers and Mathematics with Applications, 60: 660 – 669.
12. Okedoye, A. M. and Asibor, R. E. (2014). Effects of Variable Viscosity on magneto-hydrodynamic flow near a stagnation point in the presence of heat generation/absorption. J of NAMP, 27: 171 - 178
13. Okoro, F. M. and Asibor, R. E. (2016). Unsteady magneto-hydrodynamic electro-osmotic fluid flow and heat transfer analysis in a horizontal channel. Journal of the Nigerian Association of Mathematical Physics, 38: 99 – 108
14. Probstein, R. F. (2003). Physicochemical Hydrodynamics: An Introduction, Second edition, Wiley Interscience, Hoboken, New Jersey, USA.
15. Reuss, F. F. (1809). Sur un nouvel effet de l’´electricit´e glavanique M´emoires de la Societ´e Imperiale des Naturalistes de Moscou, 2: 327– 337.
16. Rice, C. L. and Whitehead, R. (1965). Electrokinetic flow in a narrow cylindrical capillary. Journal of Physical Chemistry, 69: 4017–402.
17. Smoluchowski (1903). Contribution a la theorie de l'endosmose electrique et de quelques phenomenes correlatifs. Bulletin International de l'Academie des Sciences de Cracovie, 182-200.
18. Smoluchowski, V. M. (1921). Handbuch der Elektrizitat under Magnetismus II, 2: 366-428.
19. Tanner, R.I. (2000). Engineering Rheology. Oxford University Press, New York.

Published By:
Blue Eyes Intelligence Engineering and Sciences Publication (BEIESP)

20. Whitesides, G. M. (2006). The origins and the future of microfluidics. Nature, 442: 368-373.
21. immerman, W., Rees, J. and Craven, T. (2006). Rheometry of non-Newtonian electrokinetic flow in a microchannel T-junction. Microfluidics and Nanofluidics, 2: 481-492.

APPENDIX

$$h_0(y)=\frac{Sc\pm\sqrt{Sc^2+4ScKr}}{2} \qquad h_0(y)=e^{-m_1 y}$$

$$B=\frac{AScm_1}{m_1^2-Scm_1-(Kr+n)Sc}$$

$$m_1=\frac{Sc+\sqrt{Sc^2+4ScKr}}{2}$$

$$m_2=\frac{Sc+\sqrt{Sc^2+4(Kr+n)Sc}}{2}$$

$$m_3=\frac{\Pr+\sqrt{\Pr^2+4\Pr Q}}{2}$$

$$m_4=\frac{\Pr+\sqrt{\Pr^2+4\Pr(Q+n)}}{2} \qquad m_5=\frac{1+\sqrt{1+4N}}{2}$$

$$m_6=\frac{-1+\sqrt{1+4(N+n)}}{2}$$

$$D=\frac{-\Pr\chi}{m_1^2-\Pr m_1-\Pr Q} \qquad D=1-C_5$$

$$C_5=1-D$$

$$C_7=1+\left(\frac{C_5m_3A\Pr}{m_3^2-\Pr m_3-\Pr(Q+n)}\right)+\left(\frac{-C_3\Pr\chi}{m_2^2-\Pr m_2-\Pr(Q+n)}\right)+\left(\frac{(1-C_5)A\Pr m_1-(1-C_3)\Pr\chi}{m_1^2-\Pr m_1-\Pr(Q+n)}\right)$$

$$C_9=\frac{C_5m_3A\Pr}{m_3^2-\Pr m_3-\Pr(Q+n)}$$

$$C_{10}=\frac{-C_3\Pr\chi}{m_2^2-\Pr m_2-\Pr(Q+n)}$$

$$C_{11}=\frac{(1-C_5)A\Pr m_1-(1-C_3)\Pr\chi}{m_1^2-\Pr m_1-\Pr(Q+n)}$$

$$C_{12}=\frac{Gr(1-C_5)-G_m}{m_1^2-m_1-N}+\frac{G_rC_5}{m_3^2-m_3-N}$$

$$C_{14}=\frac{-\left[Gr(1-C_5)-G_m\right]}{m_1^2-m_1-N}$$

$$C_{15}=\frac{-G_rC_5}{m_3^2-m_3-N}$$

$$C_{18}=\frac{Am_1C_{14}-GrC_{11}-Gm(1-C_3)}{m_1^2-m_1-(N+n)}$$

$$C_{19}=\frac{GmC_3-GrC_{10}}{m_2^2-m_2-(N+n)}$$

$$C_{20}=\frac{Am_3C_{15}-GrC_9}{m_3^2-m_3-(N+n)}$$

$$C_{21}=\frac{-GrC_7}{m_4^2-m_4-(N+n)}$$

$$C_{22}=\frac{Am_5C_{12}}{m_5^2-m_5-(N+n)}$$

AUTHOR PROFILE

Dr Asibor Raphael Ehikhuemhen, Ph.D in Computational Fluid Dynamics. Has his Master's degree from Olabisi Onabanjo University, Ago-Iwoye Ogun State. And a Doctor of Philosophy in Mathematics from the prestigious Ambrose Alli University, Ekpoma, Edo State, Nigeria. A researcher in Combustion, Blood flow, Electro-osmotic flow, Medical Physics. Mathematical modeling, A member of IAENG, NAMP, MAN etc. Currently the Chairman, Igbinedion University Data Committee. +2348034331960.

Mr Asibor Victor Osemudiamhen a young researcher of University of Abuja Nigeria. His research interest include amongst others, Mechanics, Thermal Physics, Electromagnetics and Modern Physics. +2348128741191.

Published By:
Blue Eyes Intelligence Engineering
and Sciences Publication (BEIESP)